Available online at www.sciencedirect.com

ScienceDirect

Procedia Engineering 101 (2015) 552 – 560

Procedia Engineering

www.elsevier.com/locate/procedia

3rd International Conference on Material and Component Performance under Variable Amplitude Loading, VAL2015

# Mechanical property change in the region of very high-cycle fatigue

Zhihong Xiong[a]*, Takashi Naoe[b], Tao Wan[b], Masatoshi Futakawa[b], Katsuhiro Maekawa[a]

[a]*Graduate School of Sicience and Engineering, Ibaraki University, 4-12-1, Nakanarusawa, Hitachi, Ibaraki 391-8511, Japan*
[b]*J-PARC Center, Japan Atomic Energy Agency, 2-4, Shirane, Shirakata, Naka-gun, Tokai-mura, Ibaraki 319-1195, Japan*

**Abstract**

Very high-cycle fatigue behaviour of type 316L austenitic stainless steel, which is used as the structural material of the pulsed spallation neutron sources, was investigated through the ultrasonic fatigue test with the strain rate of $10^2$ 1/s. Cross-sectional hardness distributions of the fatigue-failed specimens for solution annealed (SA) and cold worked (CW) 316L were measured to understand the cyclic hardening or softening in the very high-cycle fatigue region. In addition, the tensile tests of the fatigue-failed specimens were performed at room temperature. Furthermore, the nonlinear ultrasonic system was used for evaluating the dislocation density variation during plastic deformation. The results showed the cyclic hardening in the region of very high-cycle fatigue in the case of SA 316L. In contrast, in the case of 10% CW 316L, cyclic softening occurred when the number of cycles below $10^6$ and followed by cyclic hardening. In the case of 20% CW 316L, cyclic softening was observed when the number of cycles below $10^7$, while cyclic hardening occurred subsequently.


Peer-review under responsibility of the Czech Society for Mechanics

*Keywords:* Very high-cycle fatigue; Mechanical property; Ultrasonic fatigue test; Cyclic hardening; Cyclic softening; Stainless steel 316L; Dislocation density

## 1. Introduction

In modern industry, many mechanical components, such as turbine engine, railway, reactor and spallation neutron source, usually bear very-high cyclic loading (in excess of $10^8$ cycles) with high frequency and low stress amplitude. Those components require not only high strength but also excellent fatigue properties. Many researchers have focused

* Zhihong Xiong. Tel.:+81- 029-284-3716; fax: +81-029-282-6712.
*E-mail address: xiong.zhihong@jaea.go.jp*


Peer-review under responsibility of the Czech Society for Mechanics
doi:10.1016/j.proeng.2015.02.066

on investigating the very high-cycle fatigue properties of the component structural materials. It was reported that the very high-cycle fatigue degradation behavior is different from that of the conventional fatigue up to million cycles, the fatigue crack initiation due to internal flaw and/or inclusion becomes dominant in the very high-cycle fatigue regime[1, 2]. Type 316L austenitic stainless steel has been used for the structural material of the enclosure vessel of liquid mercury target for the MW-scale spallation neutron source in the J-PARC (Japan Proton Accelerator Research Complex). The target vessel suffers cyclic loading during the operation and the total number of cycles in the service life is higher than $2\times10^8$, with a high strain rate of 50 1/s at maximum under intensive proton and neutron irradiation environments[3]. Therefore, the resistance to very high-cycle fatigue is an essential requirement to evaluate the structural integrity of the target vessel.

It is well-known that empirical relationships among the fatigue strength, the ultimate strength and the hardness are described as follows[4],

$$\sigma_w = \mathrm{C}_1\sigma_u = \mathrm{C}_2 H \tag{1}$$

where $\sigma_w$, $\sigma_u$ and $H$ are the fatigue strength, ultimate tensile strength and hardness, respectively. $C_1$ and $C_2$ are the constants depending on the material. It is indicated that the fatigue strength of metals and their alloys is dependent on their ultimate tensile strength and hardness. There are many investigations on changes in mechanical properties during the cyclic plastic deformation [5-11]. The cyclic hardening for normal materials[5-6] and cyclic softening for the previously plastically-deformed materials[7-9] in the low cycle strain-controlled fatigue were observed. It was supposed that the cyclic behaviour, i.e. cyclic hardening or softening, is related to the dislocation density of the materials[10,11]. The storage-recovery model, i.e. the interaction between the plastic deformation induced dislocation generation and annihilation, was used to describe the dislocation density variation during the cyclic plastic deformation [11]. However, mechanical properties changes in the very high-cycle regime are rarely investigated.

In addition, ultrasonic diagnosis which has been used for evaluating the creep damage or cavitation damage[13,14], etc., is used to evaluate dislocation density by measuring the ultrasonic damping. The ultrasonic damping will occur due to the internal defects induced dissipated acoustic energy[13,14].

The main purpose of this paper is to study the mechanical properties in the very high-cycle regime. From this viewpoint, two parameters, micro-hardness and the residual strength, i.e. the ultimate tensile strength of the fatigue-failed specimens are measured to understand the change of mechanical properties during the cyclic plastic deformation. Additionally, the dislocation density variation during cyclic plastic deformation was investigated by using the nonlinear ultrasonic system.

## 2. Experimental procedures

### *2.1. Specimen*

The type 316L austenitic stainless steel was used for the very high-cycle fatigue test. A part of as-received materials, which were heat-treated at 1055 ºC for 6 min with water quench (referred to SA), were subjected to different cold-rolled levels, i.e. 10% and 20% reduction of thickness (referred to 10% CW and 20% CW). The original ultimate tensile strength of SA, 10% CW and 20% CW are 649 MPa, 775 MPa and 882 MPa, respectively. The original universal hardness of SA, 10% CW and 20% CW are 2.44 GPa, 4.21 GPa and 5.31 GPa, respectively.

An hourglass shape specimen was selected for the test as shown in Fig. 1(a). In order to obtain the resonance frequency of the specimen at 20 kHz, the lengths of $l$ and $L$ were selected as 22.7 mm and 40 mm, respectively. The surface roughness $R_Z$ (JIS-B6001 2001) of the as-received specimen is 2.4 μm, which is proved to have no effect on the fatigue strength[3].

### *2.2. Fatigue test*

Fatigue tests were conducted by using an ultrasonic fatigue testing system (Shimadzu, USF-2000) as shown in

Fig. 2. The specimen was loaded in tension-compression (the ratio of stress $R = \sigma_{max} / \sigma_{min}$ was -1) with a resonance frequency of 20 kHz. Fatigue failure of the specimen was defined as the resonance frequency exceeded ±500 Hz of the initial state, which was automatically detected by computer software. The maximum number of load cycles was $10^9$. This means that the specimen is not completely broken after the fatigue test.

In order to prevent the increase of specimen temperature caused by the internal heat generation together with high-speed deformation, loading/arresting intervals were controlled during the test in addition to the air-cooling of specimen surface. The temperature rise of the specimen surface was monitored by using an infrared radiation thermometer (KEYENCE, IT2-02). Its spot diameter was about 1.2 mm.

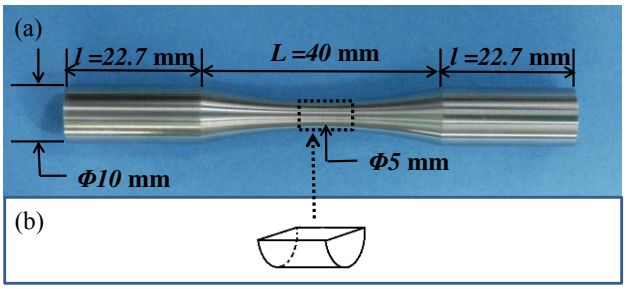


Fig. 1 Fatigue specimen (a), and hardness measurement site (b)

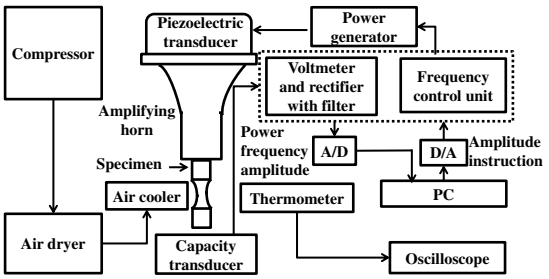


Fig. 2 Schematic of ultrasonic fatigue testing machine

### 2.3. Tensile and micro-hardness tests

As for the investigations of changes in mechanical properties by cyclic loading, the residual strength of the fatigue-failed specimen was measured through the quasi-static tensile testing machine with a crosshead velocity of 5 mm/min at room temperature. Furthermore, the cross-sectional hardness was measured by using a micro hardness tester with the Berkovich tip (Shimadzu, DUH-W201S) at the maximum load of 29.7 mN. The fatigue-failed specimen was cut in a longitudinal direction, and a centre part was used for hardness measurement as shown in Fig. 1(b). Universal hardness is defined as the quotient of the test load and the surface area of the indentation under an applied test load, which is obtained by[12]

$$H_u = \frac{L_{\max}}{26.43 D^2{}_{\max}} \tag{2}$$

where $D_{max}$ is the maximum depth and $L_{max}$ is the maximum load.

### 2.4. Nonlinear ultrasonic test

A nonlinear ultrasonic system was used for measuring the attenuation of the reflected waves. The nonlinear ultrasonic system mainly consists of a wave generator, a piezoelectric transducer and high pass filter. The detailed information of the system can be found in the reference[18]. The experiment was carried out as follows: 1) the generated ultrasonic waves with a certain frequency were sent into the center part of the specimen; 2) the reflected waves were received by the transducer; 3) the waveforms of the reflected waves were recorded after passing the high pass filter. Six positions along the circumference of the center part of the specimen were measured by using the nonlinear ultrasonic system after the fatigue test with a critical number of cycles (without failure). The fatigue test continued after the nonlinear ultrasonic test. These processes were repeated by using the same specimen. The excitation cycles of waveforms were 32 and the resonance frequencies of the incident ultrasonic wave were 7.9 MHz, for SA and 7.8 MHz for 10% CW and 20% CW, respectively. The fatigue tests were conducted with the stress amplitude of 190 MPa, 330MPa and 390 MPa for SA, 10% CW and 20% CW, respectively.

## 3. Results

### 3.1. S-N curves

The applied stress amplitude as a function of the number of cycles to failure (*S-N*) of SA, 10% CW and 20% CW are shown in Fig. 3. The *S-N* relationships are described by using two linear segments on log-log coordinate. The horizontal line represents the fatigue limit. The data above the fatigue limit were fitted according to the Wöhler's approach as follows,

$$\log N_f = a - b\log\sigma_a \tag{3}$$

where $\sigma_a$ is the stress amplitude, and $a$ and $b$ are constants.

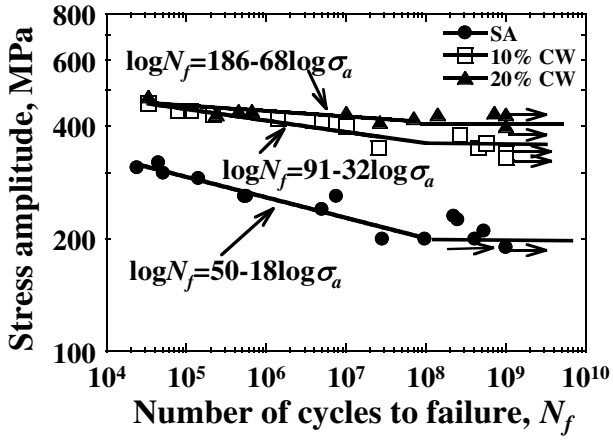


Fig. 3 S-N curves of SA, 10% CW and 20%CW

The continuous decline and stepwise *S-N* curves, which are usually observed in the very high-cycle fatigue regime for carbon steels[1, 2], were not observed in the 316L regardless of cold work. That is, there exists an obvious fatigue limit. Although the scatter is somewhat large in the case of SA, the shortest fatigue life is $2.82\times10^7$ cycles at the stress amplitude of 200 MPa. On the other hand, another specimen did not fail even beyond $4\times10^8$. The fatigue strengths of SA, 10% CW and 20% CW at the number of cycles of $10^9$ are about 190 MPa, 340 MPa and 390 MPa, respectively. The fatigue strength of 20% CW is higher than that of SA and 10% CW, and the fatigue strength was increased with CW level under the stress-controlled fatigue. The fatigue degradation rate, which is defined as the slope of the S-N curve above the fatigue limit, was increased with CW level.

### 3.2. Micro-hardness and residual strength

The residual strength and the universal hardness of fatigue-failed specimens with the different number of cycles are shown in Figs. 4 and 5. It can be seen that, in the case of SA, both of the universal hardness and the residual strength show an increase with the number of cycles: that is, a so-called cyclic hardening is recognized. In contrast, the hardness and residual strength of 10% CW show the negative relation with the number of cycles in the region below $10^6$: a so-called cyclic softening is recognized, and thereafter the cyclic hardening occurs. Furthermore, in the case of 20% CW, there exists the negative relation between the universal hardness and the number of cycles when the number of cycles

is below about $10^7$, i.e. cyclic softening occurs, thereafter the cyclic hardening is observed. The trend of the universal hardness is the same as that of 10% CW, but the break point, i.e. the cyclic hardening transit from cyclic softening, seems to shift to $10^7$ cycles approximately.

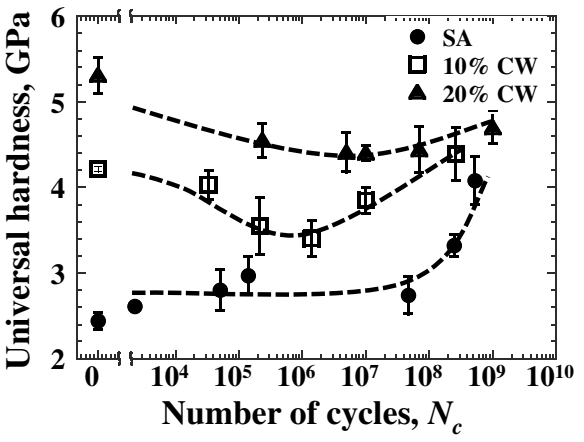


Fig. 4 Relationship between hardness and the number of cycles

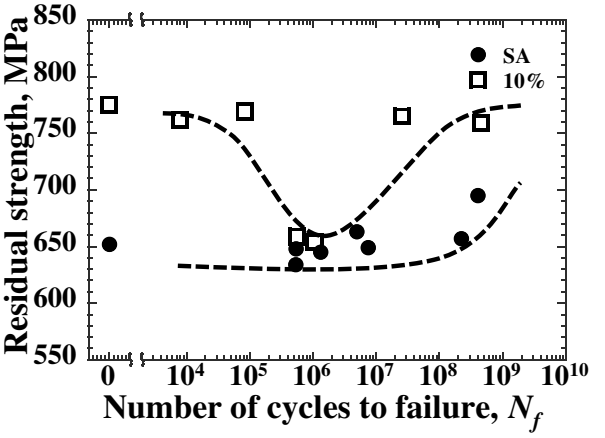


Fig. 5 Relationship between residual strength and the number of cycles

### *3.3. Damping factors*

Figure 6 shows the reflected waveforms and the damping of SA: (a) before the fatigue test, and (b) after the fatigue test. The damping factor, $\alpha$, is obtained by[14]

$$A_t = A_0 e^{-\alpha t} \tag{4}$$

where $A_0$ is the amplitude of the reflected waveform when damping starts, $A_t$ is the amplitude of reflected waveform at a certain time $t$ from the beginning of the damping. The damping factors of SA before and after the fatigue test with the number of cycles of $5\times10^4$ are 0.003 and 0.005, respectively. It is shown that the damping factor becomes larger after the fatigue test.

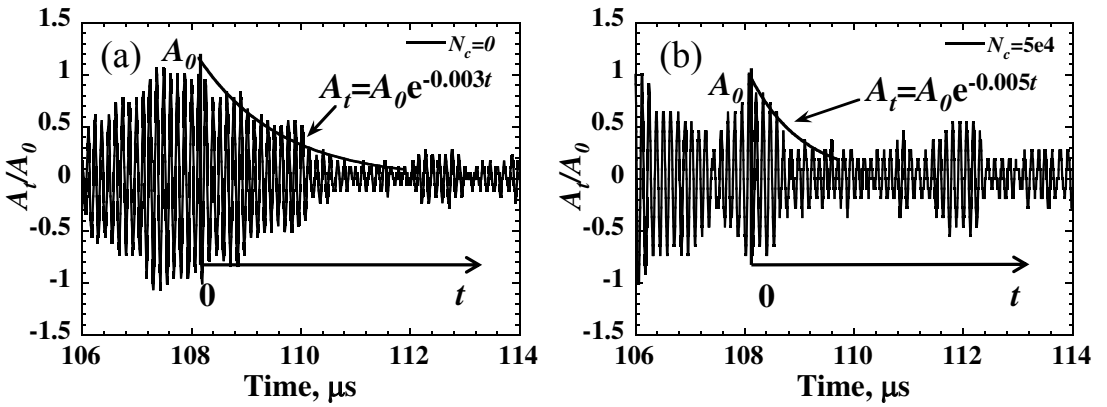


Fig. 6 Reflected waveforms and damping of SA: before the fatigue test (a), and after the fatigue test with the number of cycles of $5\times10^4$ (b)

The average damping factor, $\alpha_{ave}$, was obtained from the results of the six positions. The relations between the average damping factors and the number of cycles are shown in Fig. 7. The results indicate that, in the case of SA, the

damping factor shows an increase with the number of cycles. On the other hand, 10% CW shows the negative relation between the average damping factor and the number of cycles in the region below $10^6$, and followed by the positive relationship. Furthermore, 20% CW exhibits the negative relation between the average damping factor and the number of cycles in the region below $10^7$, and followed by the positive relation.

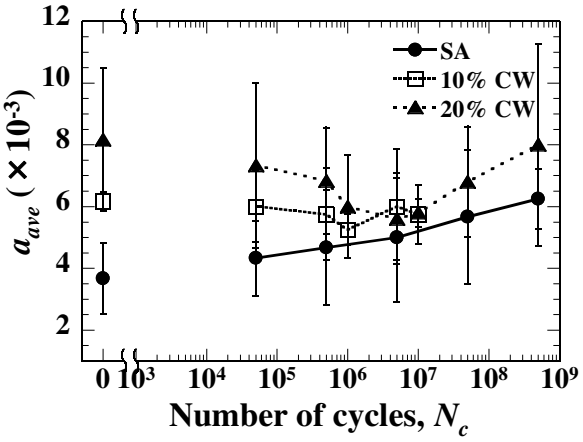


Fig. 7 Average damping factors as a function of the number of cycles

## 4. Discussion

### *4.1. Hardness and damping factor*

It is supposed that the dislocation density shows a positive relation with the CW levels[19]. The fatigue strength of metals and alloys depends on their mechanical properties, such as ultimate tensile strength and hardness. In general, the increasing in ultimate tensile strength and hardness is associated with the increment of dislocation density. Accordingly, the fatigue strength could be increased with the increase of dislocation density. And the cyclic behavior is related to dislocation density of the material[12,13]. That is, dislocation density plays an important role in the fatigue behavior of material.

Dislocation density was not measured directly in this research. However, the variation trend of dislocation density during the cyclic plastic deformation can be evaluated by the following two approaches. The first one is the hardness related to the dislocation density. The relationship between the hardness, $H$ and dislocation density, $\rho$ is expressed by[15]

$$\sqrt{\rho} = \frac{H - A}{B} \tag{5}$$

where $A$ and $B$ both are constants. For example, $A$ is 157 and $B$ is $3.03 \times 10^{-6}$ in the Vickers hardness measurement of AISI 316[16]. The second one is the damping factor of the reflected wave variation trend. The relationship between the dislocation density and the damping factors is reported to be described as follows [13],

$$\alpha = A_1 \rho L^4 f^2 \tag{6}$$

where $A_1$ is a positive constant, $L$ is the dislocation loop length, $f$ is the frequency of the ultrasonic wave.

According to Eqs. (5) and (6), the trends in variations of hardness and damping factors indicate the dislocation density dependency. Based on the results shown previously in Section 3, it can be said that SA exhibits a positive relation between the dislocation density and the number of cycles. In contrast, CW shows a negative relation between dislocation density and the number of cycles in the region below a critical number of cycles, $N_c$, whereas it shows a positive relation in the region beyond $N_c$. Note that the value of $N_c$ is dependent on the CW levels, which is about $10^6$ for 10% CW and $10^7$ for 20% CW, respectively.

Indeed, the quasi-static loading due to thermal strain has to be taken into account because the temperature increases during ultrasonic fatigue tests and varied by the air cooling with different frequency from the ultrasonic vibration for fatigue tests. In the future we will consider the effect of quasi-static superimposed loadings on the very high-cycle fatigue.

### *4.2. Dislocation density variation during cyclic fatigue*

It has been reported there are two mechanisms contributing to the dislocation density variation during cyclic plastic deformation[9,11]: on one hand, dislocations generated during the cyclic plastic deformation, which can be called as $D_{gen}$, on the other hand, dislocations are annihilated: i.e. the dislocations with opposite burgers vector (dislocation dipole, referred to $D_{dip}$) on the same glide plane may glide towards each other. This phenomenon occurs in the course of the recovery process during cyclic plastic deformation. It should be noted that there are two kinds of $D_{dip}$, one kind is the pre-existed $D_{dip}$ (referred to $D_{p\text{-}dip}$), the other one is the generated during cyclic plastic deformation (referred to $D_{gen\text{-}dip}$).

Therefore, the dislocation density variation results from the interaction between the dislocation generation rate ($r_{gen}$) and annihilation rate ($r_{ann}$). If the $r_{gen}$ is greater than the $r_{ann}$, the dislocation density will increase. Otherwise, it decreases. It was supposed that both of the $r_{gen}$ and $r_{ann}$ are proportional to the dislocation density[9,11]. From the view point of the mechanism of the dislocation annihilation, $r_{ann}$ should depend on the density of the $D_{dip}$.

In the case of well-annealed material, as the recovery process should finish during annealing, the density of $D_{p\text{-}dip}$ should be close to zero. Accordingly, the dislocation annihilation mainly attributes to the $D_{gen\text{-}dip}$. In general sense, the density of $D_{gen\text{-}dip}$ is smaller than that of the $D_{gen}$, the dislocation density shows a positive relation with the number of cycles[6,10].

On the other hand, in the case of CW, the pre-existed dislocation density is high and dislocations distribute randomly, it is reasonable that the density of the $D_{dip}$ is high, which will lead to a high $r_{ann}$. In general, as $r_{gen}$ is smaller than $r_{ann}$, the dislocation density shows a negative relation with the number of cycles[7-9]. As discussed in last paragraph, the $r_{gen}$ of $D_{gen\text{-}dip}$ is smaller than that of $D_{gen}$, so this decrement of dislocation density mainly attributes to the $D_{p\text{-}dip}$s. Since the density of $D_{p\text{-}dip}$ decreases induced by the recovery process during the cyclic plastic deformation, it is reasonable to predict that, at a critical number of cycles ($N_c$), the decrement of dislocation density will be zero: i.e. the $r_{ann}$ will be equal to the $r_{gen}$. After that, the generation of dislocation governs the variation of the dislocation. As a results, the dislocation density increases with the number of cycles.

As discussed above, the dislocation density variation of the materials dependent on their initial state, deformed or un-deformed. So we can describe the dislocation variation during cyclic plastic deformation as schematically shown in Fig. 8. In the case of SA, the dislocation density variation is governed by dislocation generation, the dislocation density shows a positive relation with the number of cycles (represented by solid curve A in Fig. 8). On the other hand, in the case of CW, when the number of cycles is below $N_c$, dislocation density variation is governed by dislocation annihilation, the dislocation density shows a negative relation with the number of cycles, and followed by a positive relation (represented by solid curve B in Fig. 8). Note that $\rho_{0,\,SA}$, and $\rho_{0,\,CW}$ in Fig. 8 are the initial dislocation density of SA and CW, respectively. Besides, the critical number of cycles, $N_c$, is dependent on the CW levels.

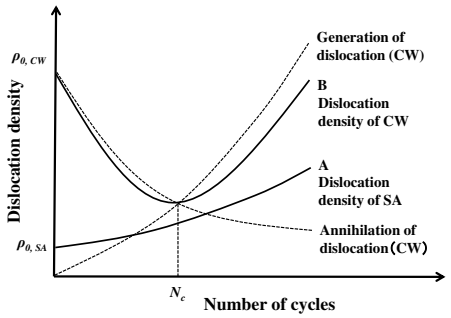


Fig. 8 Schematic diagram of dislocation density variation during cyclic loading

## 5. Conclusion

In this paper, fatigue tests were conducted by using the ultrasonic fatigue testing system. The micro-hardness, the residual strength and the damping factors of SA, 10% CW and 20% CW were measured in order to investigate changes in the mechanical properties in the very high-cycle fatigue.

The results showed that the re-degradation of the fatigue limit was not observed in the very high-cycle regime, and the fatigue strength was increased with the CW level. The cyclic behaviours of the materials are dependent on their initial state, deformed or un-deformed. In the case of solution annealed (SA) 316L, both of the universal hardness and residual strength showed a positive relation with the number of cycles: i.e. cyclic hardening occurred. On the contrary, in the case of cold worked (CW) 316L, both of the universal hardness and residual strength showed a negative relation with the number of cycles when the number of cycles smaller than a critical value and subsequent hardening was observed. The critical number of cycles is about $10^6$ for 10% CW and $10^7$ for 20% CW, respectively.

It is deduced from the nonlinear ultrasonic testing results that the dislocation density increased with the number of cycles in the case of SA. In contrast, CW specimens show a negative relation between dislocation density and the number of cycles in the region below the critical number of cycles, thereafter it shows a positive relation.

## Acknowledgement

This research was partly supported by Japan Society for the Promotion of Science through a Grant-in- Aid for Scientific Research (No. 23360088 and 26820016 ).

## Reference

[1] T. Sakai, Review and prospects for current studies on very high cycle fatigue of metallic materials for machine structural use, J. Solid Mech. Mater. Eng. 3(2009) 425-439.

[2] S.X. Li, Effects of Inclusions on very high cycle fatigue properties of high strength steels, Int. Mater. Rev.. 27(2012) 92-110.

[3] Z.H. Xiong, M. Futakawa, T. Naoe, K. Maekawa, Very High cycle fatigue in pulsed high power spallation neutron source, Adv. Mater. Res.. 891-892(2014) 536-541.

[4] A. Casagrande, G.P. Cammarota, L. Micele, Relationship between faituge limit and Vichers hardness in steels, Mater. Sci. Eng. A. 528(2011)3468-3473.

[5] D. Yu, K. An, Y. Chen, X. Chen, Revealing the cyclic hardening mechanism of an austenitic stainless steel by real-time in situ neutron, Scripta Mater.. 89(2014) 45-48.

[6] H. Mughrabi, The cyclic hardening and saturation behavior of copper singe crystals, Mater. Sci. Eng.. 33(1978)207-223

[7] S.G. Hong, et al., The tensile and low-cycle fatigue behavior of cold worked 316L stainless steel: influence of dynamic strain aging, Int. J. Fatigue. 26 (2004) 899-910.

[8] S.G. Hong, S. Yoon, S.B. Lee, The effect of temperature on low-cycle fatigue behavior of prior cold worked 316L stainless steel, Int. J. Fatigue. 25 (2003) 1293-1300.

[9] M.S. Pham, S.R. Holdsworth, K.G.F. Janssens, E. Mazza, Cyclic plastic deformation response of AISI 316L at room temperature: Mechanical behavior, microstructural evolution, physically-based evoluationary constitutive modelling, Int. J. Plasticity. 47(2013) 143-164.

[10] R.I. Stephens, A. Fatemi, R. R. Stephens, H.O. Fuchs, Metal Fatigue in Engineering, second ed., John Wiley & Sons, Inc, New York. 2001.
[11] E.I. Galindo-Nava, J. Sietsma, P. E. J. Rivera-Díaz-del-Castillo, Dislocation annihilation in plastic deformation: II. Kocks-Meching analysis, Acta. Materialia. 60 (2012) 2615-2624.
[12] W. Weiler, The relationship between vickers hardness and universal hardness, The proceedings of the 79th AESF annual technical conference, AESF. Inc., Atalanta, 1992, pp. 277-284.
[13] T. Ohtani, H. Ogi, M. Hirao, Dislocation damping and microstructural evolutions during creep of 2.25Cr-1Mo Steels, Metall. Mater. Trans A. 36(2005) 411-420.
[14] T. Wan, T.Wakui, T. Naoe, M. Futakawa, K. Maekawa, A novel ultrasonic evaluation process for cavitaiton damage by conbination of attenuation and higher harmonics, JSEM. 13(2013) 387-394.
[15] S. Takaki, T. Tsuchiyama, K. Nakashima, H. Hidaka, K. Kawasaki, Y. Futamura, Microstructure development of steel during severe plastic deformation, Mat. Mater. Int.. 10(2004) 533-539.
[16]M. Kumagai, K. Akita, M. Imafuku, S. Ohya, Workhardening and the microstructural characteristics of shot- and laser-peened austenitic stainless steel, Mater. Sci. Eng. A. 608(2014)21–24.